Demonstration of a segment alignment maintenance system on a seven-segment subarray of the Hobby-Eberly Telescope

Rakoczy, John, Hall, Drew, Howard, Richard, Weir, John, Montgomery, Edward, et al.

John M. Rakoczy, Drew Hall, Richard T. Howard, John T. Weir, Edward E. Montgomery IV, Gregory H. Ames, Tim Danielson, Phil Zercher, "Demonstration of a segment alignment maintenance system on a seven-segment subarray of the Hobby-Eberly Telescope," Proc. SPIE 4494, Adaptive Optics Systems and Technology II, (4 February 2002); doi: 10.1117/12.454780

SPIE.

Event: International Symposium on Optical Science and Technology, 2001, San Diego, CA, United States

Demonstration of a Segment Alignment Maintenance System on a seven-segment sub-array of the Hobby-Eberly Telescope

John Rakoczy, Drew Hall, Richard Howard, John Weir, Edward Montgomery
NASA Marshall Space Flight Center
Huntsville, Alabama

Greg Ames, Tim Danielson, Phil Zercher
Blue Line Engineering
Colorado Springs, Colorado

ABSTRACT

NASA's Marshall Space Flight Center, in collaboration with Blue Line Engineering of Colorado Springs, Colorado, is developing a Segment Alignment Maintenance System (SAMS) for McDonald Observatory's Hobby-Eberly Telescope (HET). The SAMS shall sense motions of the 91 primary mirror segments and send corrections to HET's primary mirror controller as the mirror segments misalign due to thermo-elastic deformations of the mirror support structure. The SAMS consists of inductive edge sensors. All measurements are sent to the SAMS computer where mirror motion corrections are calculated. In October 2000, a prototype SAMS was installed on a seven-segment cluster of the HET. Subsequent testing has shown that the SAMS concept and architecture are a viable practical approach to maintaining HET's primary mirror figure, or the figure of any large segmented telescope. This paper gives a functional description of the SAMS sub-array components and presents test data to characterize the performance of the sub-array SAMS.

Keywords: edge sensors, figure maintenance, segmented mirrors, active optics

1. INTRODUCTION

The Hobby-Eberly Telescope (HET) is a 9.2-m fixed elevation telescope with a segmented primary mirror. It is located at McDonald Observatory in far West Texas at an elevation of 2,008m. Descriptions of the telescope and its operation, may be found at the indicated references[1,2]. A cutaway view of the facility with its major components is shown in Figure 1. Telescope commissioning was completed in early October 1999.

The HET employs a spherical segmented primary mirror supported by a steel truss as an essential part of the telescope's low-cost, Arecibo-style design concept (see Figure 1). The unique design of the HET allows the primary mirror to remain stationary during an observation; it

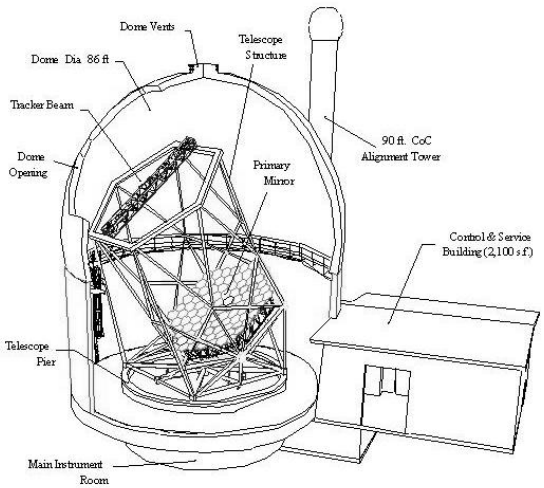

Figure 1: Hobby-Eberly Telescope

Adaptive Optics Systems and Technology II, Robert K. Tyson, Domenico Bonaccini, Michael C. Roggemann, Editors, Proceedings of SPIE Vol. 4494 (2002)

can be rotated and repositioned in azimuth between observations to access different areas of the sky. The mirror has a constant zenith angle of 35 degrees, and thus always has the same orientation with respect to gravity. Images of astronomical objects are acquired and followed across the mirror array at prime focus for up to 2.5 hours by means of a tracking device (Tracker Beam in Figure 1, above) mounted atop the telescope structure.

HET first light was achieved in December 1996 with seven mirror segments collecting and focusing light through a test optical corrector. During initial testing of the telescope after first light, composite star image spots formed by individual mirror segments were observed to "de-stack", or move with respect to each other, over a period of time after the segments had been "stacked", or aligned with each other. While minor segment motion over a period of an hour or more had been anticipated in the original design, misalignment of the segments on a time scale of tens of minutes under some conditions was unexpected.

In November 1999, the University of Texas at Austin entered into a Space Act Agreement with NASA's Marshall Space Flight Center to procure a Segment Alignment Maintenance System (SAMS) for the HET[3,4]. The objective of the SAMS is to correct the effects of the de-stacking phenomenon, maintaining primary mirror segment alignment to within the following specifications: root mean square (RMS) tip/tilt errors to within 0.06 arcseconds, piston errors to within 15 micrometers RMS and global radius of curvature (GRoC) to within 300 micrometers. MSFC teamed with Blue Line Engineering of Colorado Springs, Colorado. Blue Line provides the edge sensing system and electronics. MSFC develops control algorithms and control system software. MSFC also oversees system integration and verification testing.

The SAMS consists of inductive edge sensors, sensor electronics, and a central control computer. A seven-segment sub-array test was required in order to prove the SAMS concept on a subscale system. This paper describes the SAMS hardware and software prototypes, which were installed on a seven-segment sub-array of the HET in October 2000. This paper also presents quantitative results of performance testing conducted on the sub-array through April 2001. The test results indicate that the SAMS is a viable practical solution to figure maintenance of large segmented primary mirrors.

2. SYSTEM DESCRIPTION

2.1 Edge Sensors

At the heart of the SAMS are the inductive edge sensors. The inductive edge sensor requires that pairs of inductors be deposited on the opposite edges of the neighboring segments. One pair of these inductors is referred to as the "Passive" side since it requires no power and is not physically connected to the other pair of coils. The other pair is referred to as the "Active" side. These two pairs of coils, or the active and passive sides of the sensor, are separated by the gap between adjacent segments. They are located on the opposing faces of these segments such that they are geometrically opposite to each other when the two segments are properly aligned. The geometric relationship of these four coils is the key to the behavior of the transducer. (See Figure 2)

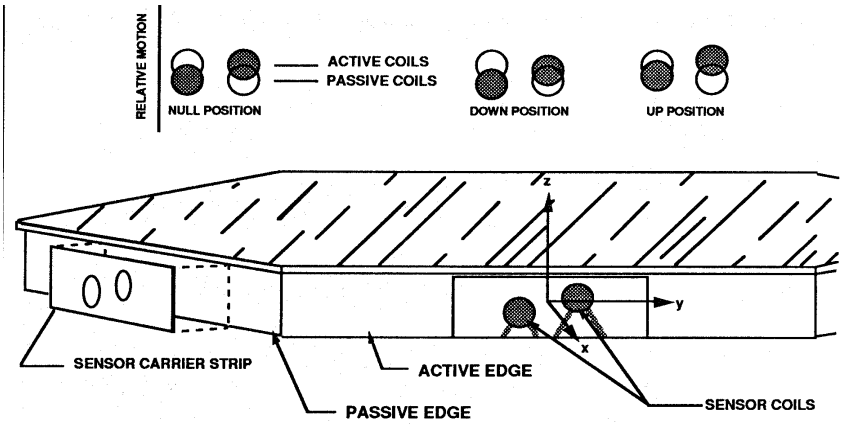

Figure 2: Edge sensor placement

The two "Active" sensing elements are series connected to form an RLC-network, which is driven by a frequency-stabilized source. The two active coils are also inductively coupled to the two "Passive" coils, which are connected to form two completely passive LC networks. The arrangement of the coils is such that any relative motion of the adjacent edges in the direction orthogonal to the mirror surfaces will cause a change in the complex impedance of the active coils. This impedance change is detected with a synchronous demodulator to produce a voltage signal. The voltage signal is linearly related to the relative motion, or edge match error, between segment edges.

Figure 3 shows the locations of the active and passive coils on a 7-segment sub-array of the HET. The 'x' denotes the active coils, and the 'o' identifies the passive coils. The photo in Figure 3 shows the actual edge sensor assemblies on the HET sub-array. HET's requirement on SAMS for tip/tilt maintenance is 0.06 arcseconds RMS. That requirement flows down to an edge sensor shear displacement accuracy requirement better than 50 nanometers RMS.

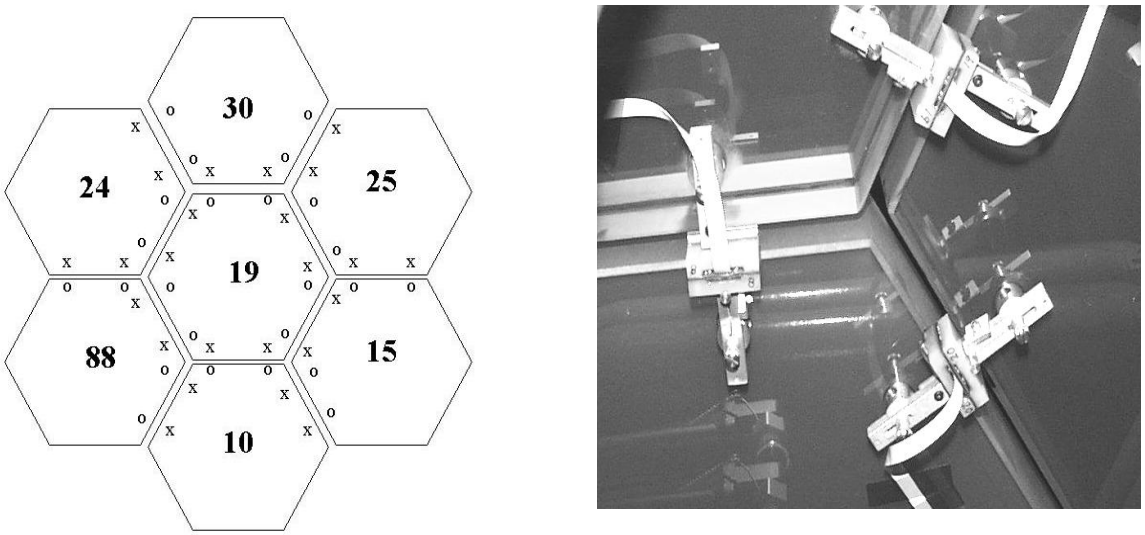

Figure 3: Edge sensor placement on HET sub-array

2.2 System Processing Architecture

The system processing architecture consists of a modified version of Blue Line's Segmented Mirror Control System, which was originally developed for the Phased Array Mirror Extendible Large Aperture (PAMELA) telescope[5]. This distributed, highly modular processing system was developed to meet the challenge of closed-loop control of segmented arrays with frame rates of 5 kHz. A block diagram is presented in Figure 4.

2.3 Nodes

At the lowest level in the system architecture are the segment nodes. Each HET segment has a node. A node is actually composed of two functional elements. The first is a DSP board that performs local processing operations on the segment's sensor signals. It also sends and receives data via the serial data link to its respective Cluster Control Processor. The second functional portion of each node consists of the Edge Sensor Electronics and analog-to-digital converters. All analog-to-digital conversions and local processing of sensor signals are performed at the segment level in the nodes.

2.4 Hubs

At the next level up are the cluster hubs. The HET array is subdivided into three clusters. Two clusters have 30 segments. The third cluster has 31 segments. The Hubs serve two important functions in SAMS. They serve as the main branching point in the distribution harness for power and timing signals. The Hubs also play an essential role in the reliable transmission and reception of data to and from the segments. Downward, the hubs communicate to the segment nodes. Upward, the hubs communicate to their respective Cluster Control Processors.

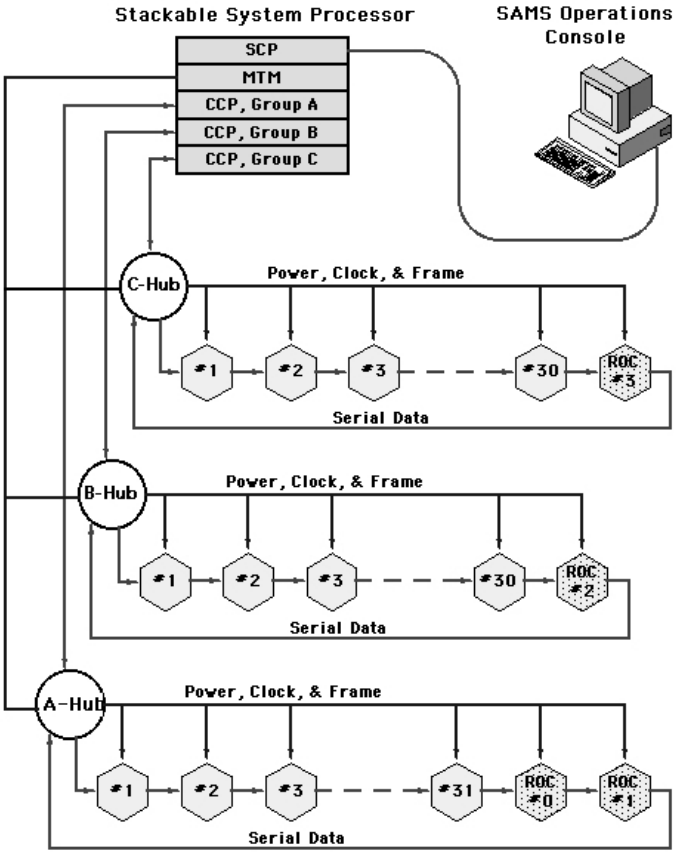

Figure 4: System processing architecture

2.5 Stackable System Processor

The Stackable System Processor (SSP) is a powerful parallel processing system that is packaged in a small, modular format. The individual modules are stacked together to build up the system as needed for the application at hand. The low power processors do not require forced air cooling so the hardware is very well suited to a wide range of field conditions. The basic building blocks are each described below and the current packaging design is shown in Figure 5.

The System Control Processor (SCP) is the gateway from the user console to the edge sensor system. The SCP provides the single-point interface to the sensor and data acquisition component of SAMS. The SCP handles all sensor-side communications. The main function of the SCP is to coordinate the operation of a bank of parallel digital signal processor based modules referred to as Cluster Control Processors (CCP) and other auxiliary modules connected to a stackable parallel data bus. The SCP also handles a wide variety of mission specific tasks as well as telemetry extraction, general health and status monitoring, downloading and initialization, and master timing control. The SCP is itself a single board computer that significantly reduces the complexity of controlling and operating the system from the user or host's perspective. It allows a very complex distributed sensing and data processing system to appear to the console user as a highly programmable intelligent instrument. In the current hardware, the SCP consists of a commercially available board, which uses a Motorola 68332 processor and measures roughly 2.5" by 8".

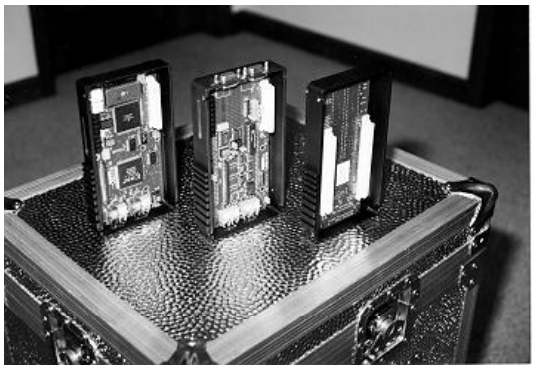
Figure 5: Stackable System Processor

The SCP communicates with the bank of Cluster Control Processors (CCP). Each CCP is a high speed dedicated processing unit, which handles the processing chores within each predefined cluster of the array. The DSP selected for the CCP module is the Motorola 56301. This 24-bit processor is capable of 80 million arithmetic operations per second. Each CCP is connected to two serial data buses (the A and the B busses).

These busses allow full duplex inter-processor communication at 22 MHz. Processor-to-processor as well as broadcast modes are available. The 56301 has 7 DMA channels, four of which may be used for inter-processor communication over the A and B busses. This allows extremely efficient inter-processor data exchanges, which do not require any on-going processor time or intervention. The most distinctive feature of the CCP is the high-speed serial data links. The design allows data to be simultaneously transmitted and received through four separate ports (2 Tx and 2 Rx ports) at bit rates as high as 10 MHz.

The Master Timing Module (MTM) was designed and developed to provide the timing signals needed for SAMS, including a 4 MHz "master clock" and a "frame sync." These signals are used to clock data through the system, and to indicate the start of a new "frame". This function is also important for two other reasons: the clock signal is used by the edge sensor system, and the frame sync sets the sample rate for SAMS. The clock signals generated by the MTM are derived from a temperature compensated crystal oscillator, and are made available to the rest of the processor modules through the stacking connector that connects the CCP boards. Fiber optic links are also provided to allow these timing signals to be sent to the segmented mirror array.

2.6 Operations Console Software

The SAMS operational software is being developed on a SUN/Solaris platform using National Instruments' LabVIEW software development tool. The SAMS software collects and stores sensor data from the SSP, implements the control system algorithm, which computes the mirror tip, tilt, and piston corrections needed to maintain the alignment of the primary mirror, and provides server functions over a standard TCP/IP interface. The SUN workstation is connected via Ethernet to a terminal server. The SSP interfaces to the terminal server via serial port.

All data into and out of the SAMS software is transferred using socket port connections over a 100BaseT LAN and conform to the TCP/IP (IP version 4) protocol and the Berkeley Socket abstraction. The SAMS software manages three server ports and one client port. One server port provides an interface for the telescope operator to use to provide configuration and control of SAMS. Another server port provides access to the mirror segment tip, tilt, and piston correction data and sensor data. The third server port provides a diagnostic interface to the lower level SAMS electronics. The client port is used to communicate with the HET's Primary Mirror Controller (PMC).

In addition to the socket port interfaces, the SAMS software provides a local interface which provides the SAMS operator the current operating mode of SAMS, a brief status of SAMS, an indication of what clients are connected, a scrollable textbox of the commands received over the socket connections, a scrollable textbox of the errors encountered, and a plot of a metric used to determine the overall performance of SAMS.

2.7 Control System Formulation

Figure 3 identifies the locations of the 24 edge sensors in the sub-array SAMS. The edge sensor architecture is designed to estimate corrections to each segment's tip, tilt and piston motions. In the configuration depicted in Figure 3, there are 24 measurements and 21 degrees of freedom (DOF). Since all angular motions are small, the equations relating the measurements to the DOFs can be simplified into a single, linear matrix equation:

$$\mathbf{y} = \mathbf{C}\mathbf{x} \qquad (1)$$

The vector y is 24 x 1 and contains the edge sensor measurements. The vector x is 21 x 1 and contains the tip, tilt and piston motions of the segments. The matrix C is the 24 x 21influence matrix relating the segment DOFs to edge sensor outputs.

The configuration in Figure 3 yields a C-matrix that has rank of 17. The four null space vectors correspond to the global tip, tilt, piston and radius of curvature modes. The original SAMS concept defined a tip, tilt and piston boundary condition on segment 19, thereby constraining the global tip, tilt and piston modes. The early concept also called for inclinometers mounted on segments 19 and 30 in order to sense a differential tilt angle between the segments and subsequently the global radius of curvature. However, preliminary testing of the baseline inclinometers revealed that those inclinometers would not satisfy the differential tilt accuracy requirement of < 0.05 arcseconds over HET's operational temperature range and over the dynamic range of segment motions.

A different boundary condition scheme was employed for the sub-array configuration. Four boundary conditions were applied to fully constrain equation 1 mathematically. Piston constraints were applied to segments 19, 30, 88 and 15. The resulting x -vector was now 17 x 1, and the C-matrix was 24 x 17 and full rank. Then a unique optimal control could be derived in order to minimize the performance metric:

$$\mathbf{J} = (\mathbf{y}_{\mathbf{ref}} - \mathbf{y})^{\mathbf{T}} (\mathbf{y}_{\mathbf{ref}} - \mathbf{y}) \qquad (2)$$

The vector y_{ref} is the 24 x 1 vector of edge sensor reference measurements. That is, y_{ref} is the vector of edge sensor measurements taken immediately after the array is stacked to the desired image quality. Then $(y_{ref} - y)$ is the error signal for the control system's feedback. The performance metric J is the global variance of all the edge sensor measurements with respect to the reference measurements. The optimal control that minimizes J, the global variance metric, is the following

$$\mathbf{u} = (\mathbf{C}^{\mathbf{T}}\mathbf{C})^{-1}\mathbf{C}^{\mathbf{T}} (\mathbf{y}_{\mathbf{ref}} - \mathbf{y}) \qquad (3)$$

The vector u is 17 x 1 and contains the control commands for the 17 active degrees of freedom. Equations 2 and 3 illustrate that the control system was designed to minimize the global edge match error of the segments in a least squares manner.

The consequence of the choice of the four boundary conditions was that the control system would always try to match up the edges of the sub-array segments to the reference sphere defined by the piston positions of segments 19, 30, 88 and 15. Unfortunately, segments 19, 30, 88 and 15 do not remain fixed in piston. The segments are vulnerable to the same dynamics as any other segment. Relative motions among the boundary conditions result in changes in the radius of the reference sphere. SAMS is required to maintain HET's GRoC to within 300 micrometers of its reference. 300 microns of GRoC change converts to a tolerance of 218 nanometers of relative motion among the four boundary conditions.

Since the actual relative boundary condition motions were unknown, the risk associated with the four-point boundary condition and its accompanying 218-nanometer tolerance was accepted for the sub-array test. In the event that boundary condition motions exceeded the tolerance, a provision was made in the control system software to occasionally enter a GRoC "joystick" command. The joystick command enabled the SAMS operator to enter a change in global radius sign and magnitude with a single external command, much like moving a GRoC joystick. When the telescope operator observed sufficient image quality degradation, the SAMS operator would enter an appropriate GRoC command to SAMS.

3. SUB-ARRAY TEST

The sub-array SAMS hardware was installed on the telescope in October 2000. Some infant mortality problems with the electronics were corrected, and system characterization testing continued during the November and December 2000 HET engineering runs. During those test runs, the data indicated that the inclinometers were not suitable for HET's operating conditions. In January 2001 some SAMS components were removed for minor adjustments and were reinstalled in March 2001. In March characterization testing resumed with the four-point boundary condition and GRoC joysticking. The formal sub-array test (SAT) was completed in April 2001.

3.1 Sub-array Test Description

In order to demonstrate and characterize the ultimate capabilities of the sub-array SAMS, the sub-array test was conducted in as ambient an environment as possible. The telescope was rotated in azimuth to point at the Center of Curvature Alignment System (CCAS) tower. The telescope was not moved at all during the SAT except for a brief period late in the test when a celestial target was observed. When the telescope was pointed at the CCAS tower, metrology data were taken from either an imaging camera or a shearing interferometer. The intent of the sub-array test was for the telescope operator (TO) to stack the SAMS cluster once at the beginning of the test and not have to restack for seven days, allowing SAMS to maintain the primary mirror figure to the original reference. Because of the relative motions of the four boundary conditions, joysticking the GRoC was required during the seven-day test. Joysticking did not require the TO to perform the usual stacking procedure. Rather, a single man-in-the-loop GRoC error command was sent to the SAMS control system to adjust the GRoC. Also, inadequate edge sensor temperature compensation caused stack degradation, requiring the TO to restack the sub-array whenever the telescope truss's mean temperature deviated more than +/- 3 degrees from the temperature at which the sub-array was stacked. Figure 6 summarizes the main events during the seven-day test.

Date	Time CST/CDT	Event	Truss Temp. Degrees C
29-March	01:25	Stack	9.5
29-March	23:48	Unable to Restore stack	14.0
30-March	22:12	Stack	13.4
1-April	23:00	Unable to Restore Stack	18.3
2-April	0:00	Stack	18.0
5-April	02:00	Observe star	19.1
6-April	02:30	Test Complete	17.9

Figure 6: Sub-array test main event summary

The event summary indicates that the TO was required to restack the sub-array twice during the seven-day test. The restacks occurred when the telescope truss temperature change from reference was 4.5 degrees C and 4.9 degrees C, respectively. From 2 -April 0:00 through 6-April 02:30 temperature remained within a band from 15-21 degrees C. During this 98.5-hour period no restacking was required. Only 12 GRoC joystick adjustments were applied during that time. SAMS de-stacking during SAT was caused by two factors: inadequate edge sensor temperature compensation and changes in the GRoC induced by the control system. The following section describes these limiting factors to SAMS performance and then quantifies SAMS performance during optimal conditions.

3.2 Edge Sensor Drift

The first source of SAMS sub-array de-stacking is edge sensor drift. Any drift in the edge sensors shows up in the global variance, J. Recalling equation 2 above, J is the sum of the squares of all edge sensor error signals. J is also the optimal control metric, which the controller tries to minimize. The control system tries to drive the system states so that J is a global minimum. Sensor drifts give misinformation to the controller. The controller then tries to drive the system to what it thinks is a global minimum. However, the corrupted sensor signals cause it to go to some other state. Errors build up, and J begins to grow. Subsequently, overall performance degrades. SAT data were reviewed and sub-array de-stacking was correlated with growth in the global variance metric, J. SAT data indicated that J was highly correlated with temperature change. Figure 7 is just one example of the temperature correlation observed during the SAT. The abscissas in Figure 7 are sample number with respect to the labeled reference time. Edge sensors were sampled once every 1.5 seconds, and temperature was sampled once every 150 seconds. Figure 7 shows data taken in the first six hours after stacking.. During that time, while the temperature dropped from 18 down to 15 degrees C, the control system error grew.

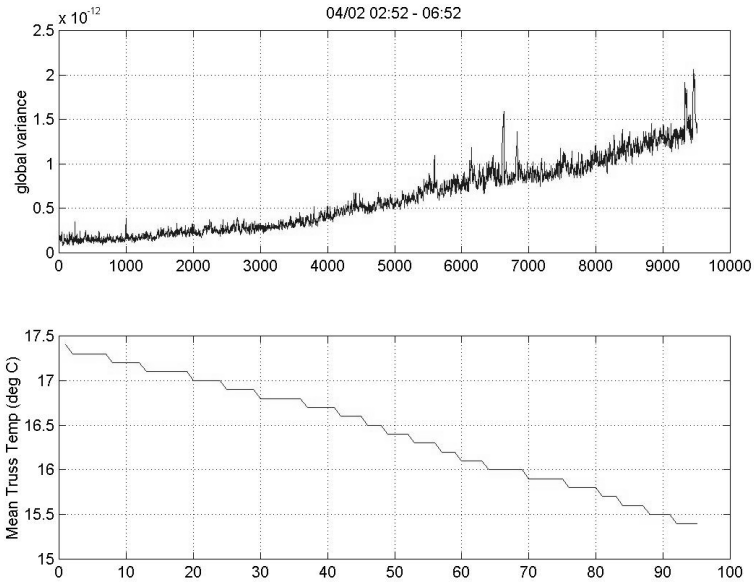

Figure 7: Global error variance & truss temperature time histories

The final value of J in Figure 7 was about 1.5e-12 at 6:52 at dome closing following a GRoC joystick command (joystick causes a brief transient). If one divides that value of J by 24 and then takes the square root, one obtains 250 nanometers per sensor (if all sensors drifted equally). Over the temperature change observed in Figure 7, the thermal drift rate is about 80 nanometers per degree C. Prior to SAT, extensive simulations were performed. Simulations indicated that sensor thermal drifts of 80 nanometers per degree C cause the same magnitude of J as was observed in Figure 7. Data were compiled throughout the SAT to show the general trend. Figure 8 plots J versus change from reference temperature during the SAT.

Figure 8 demonstrates a roughly parabolic relationship between the global variance and the departure from stack temperature. Global variance growth greater than 2e-12 coincided with a degraded image quality that could not be improved by GRoC corrections alone. When the metric was that large, the TO was required to restack the sub-array again. When the metric exceeds 2e-12, that corresponds to a per sensor drift of 287 nanometers. 287 nanometers converts to 0.12 arcseconds of tip/tilt at the mirror edge (if all that error is exclusively tip and tilt, not piston). Tip/tilt errors greater than 0.1 arcseconds RMS become visually discernible from faceplate images at the CCAS tower.

Since the test results indicated that SAMS, with edge sensors uncompensated for thermal effects, could only meet specification within a 6-degree C band, efforts were undertaken to improve edge sensor temperature compensation. Blue Line Engineering utilized SAT data to perform an *ex post facto*

temperature calibration of the edge sensors. The calibration process involved examining edge sensor measurements immediately after stacking at different temperatures. The resultant calibrations indicated local sensor drifts ranged from 30 to 100 nanometers per degree C. The magnitude of those estimated drifts agree with the 80 nanometers per degree C inferred from Figure 7 and predicted in simulation. Blue Line reported that the improved temperature compensation could open the +/- 3 degree C band out to +/- 10 degrees C. A band that large would cover most HET operational conditions.

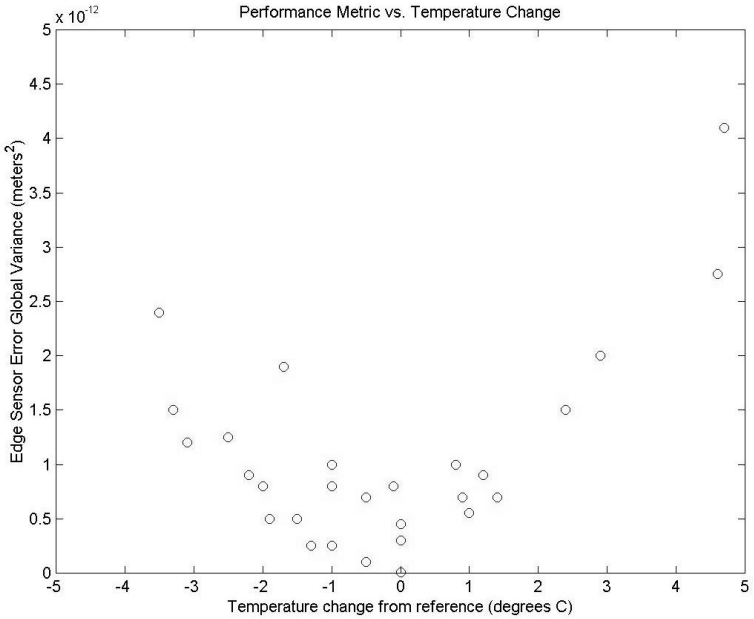

Figure 8: Global error variance vs. truss temperature change during SAT

3.3 Global Radius of Curvature Compensation

The second cause of de-stacking was an uncompensated global radius of curvature mode. Because SAMS could not observe the GRoC mode of the primary mirror, the control system could induce a GRoC mode into the primary mirror when the environment caused the uncontrolled boundary conditions to move. A 300-micrometer radius of curvature change is caused by a 0.09-arcsecond dihedral angle change of the segments. During SAT, in order to maintain the right focus position, 12 external GRoC adjustments were made. Figure 9 shows the cumulative dihedral angle that was commanded to the SAMS during the final 98.5-hour period of SAT. The total cumulative dihedral angle at the end of the test was about 2.7 arcseconds. A dihedral angle correction of 2.7 arcseconds would result from relative boundary condition motions of 6.5 micrometers. A relative piston motion of 6.5 micrometers among segments

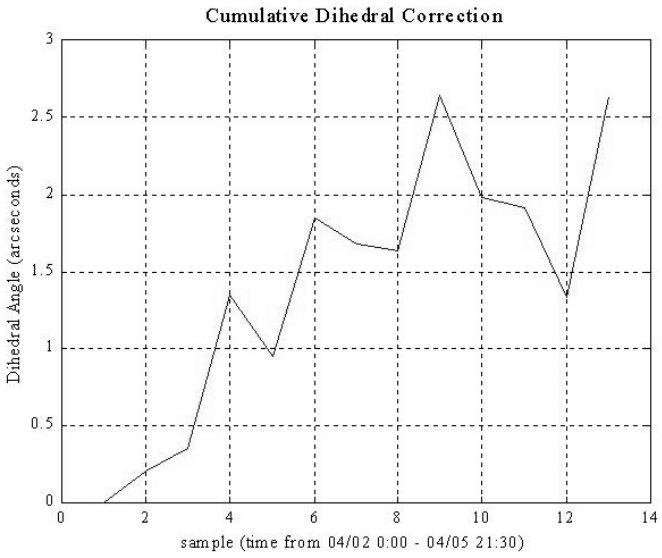

Figure 9: Cumulative GRoC correction

is not unreasonable, especially on the outskirts of the HET primary mirror.

It is expected that the control system will be less sensitive to relative boundary condition motion when the full array is populated with edge sensors. On the full array, the boundary conditions will be moved out to the third or fourth ring of hexagons. On the third ring, the tolerance is 2.0 micrometers motion per 300 micrometers GRoC change. On the fourth ring the tolerance is 3.5 micrometers per 300 micrometers GRoC change. In addition to taking advantage of the relaxed tolerance on the full array, research is underway to develop a modified edge sensor, which will sense dihedral angle. Also a GRoC estimator, which could estimate the controller-induced GRoC from accumulated control commands, is being investigated.

3.4 Sub-array Test Metrology

The above section described the limitations to SAMS performance. The next section describes the metrology and the quality of SAMS performance when temperature conditions were most favorable. While parked at the CCAS tower, three types of scoring data were obtained. One type of scoring involved using the interferometer at the CCAS tower. When the interferometer was operating, laser light was sent out a pinhole at the CCAS tower, down to the primary mirror and back through the pinhole. The shearing interferometer quantified segment tip and tilt errors. At other times the pinhole was repositioned so that a camera observing the pinhole's faceplate captured the image of the stack of spots from the primary mirror. The pinhole faceplate could be moved in and out of focus so that the image quality and focus position of the SAMS cluster could be compared to those of a single reference mirror. This latter type of scoring quantified how well SAMS was maintaining GRoC. The third scoring metric involved verification of piston performance. At the beginning of the SAT and at the end of the SAT, HET staff used a spherometer to measure the piston misalignment of each segment of the SAMS SAT cluster. The difference between the beginning and end measurements was accepted as the SAMS piston maintenance. The three scoring methods described above were intended to quantify SAMS performance with respect to the tip, tilt, piston and GRoC maintenance requirements.

The scoring data obtained from the SAT indicate that SAMS performed to specification while the temperature remained within the 6-degree temperature band noted above. The pre- and post-test piston measurements yielded a piston error of 8 micrometers RMS while the spherometer accuracy was about 6 micrometers. Measured focus positions indicated that the global radius of curvature was maintained to within 300 micrometers of the reference segment with the aid of the 12 joystick adjustments. The CCAS interferometer reported RMS tip/tilt errors of 0.08 arcseconds. The 0.08 arcseconds is barely outside the 0.06-arcsecond specification. However, CCAS tower wind-shake, bad seeing, camera noise, and a very slow sample rate (once every 2 minutes) put much of the interferometer data in question. Image quality, the ultimate metric for system performance, was maintained such that the sub-array's EE50 was less than 1.1 arcseconds at the CCAS tower for the duration of the test.

In addition to the metrology taken at the CCAS tower, data were gathered from observations of an actual celestial target. As the event summary (Figure 6) indicates, 74.5 hours after the stack performed at 2-April 0:00, HET was rotated in azimuth and the tracker started tracking a star. The target was a star of visual magnitude 14.5. Figure 10 shows an image taken by one of HET's science cameras. The picture shows three separate images of the star. One image is from a single reference segment (a 1-meter aperture), segment number 20, which was used as a focus and image quality reference. The second image is an image created by the SAMS sub-array (a 3-meter aperture). The third image is an image obtained from a seven-segment reference cluster (also a 3-meter aperture) of segments neighboring the SAMS cluster. The reference cluster was originally stacked at the same time the SAMS cluster was stacked, except the reference cluster had no figure maintenance.

The star images in Figure 10 certainly prove the mirror figure maintenance benefits gained from the SAMS. 74.5 hours after stacking, the reference cluster had broken into two separate disfigured blobs. Meanwhile, the SAMS cluster maintained a single spot with circular symmetry. Furthermore, the SAMS image had an EE50 of 1.57 arcseconds while the single reference segment had an EE50 of 1.15 arcseconds. Considering

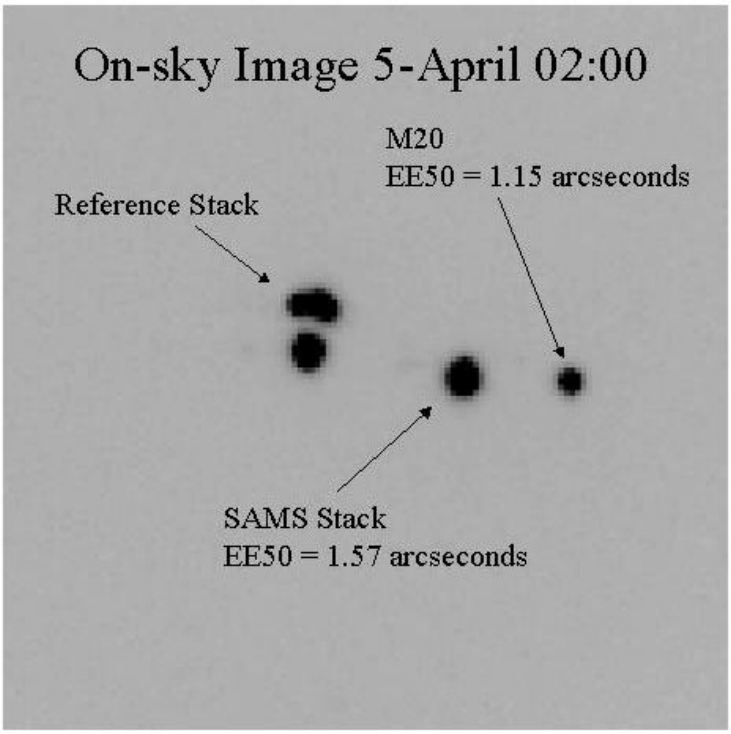

Figure 10: On-sky image from sub-array test

that segment 20 represented the median image quality of HET segments, the SAMS was maintaining its sub-array's image quality to the seeing limit.

4. CONCLUSION

In October 2000 a subscale segment alignment maintenance system (SAMS) was installed on a seven-segment sub-array of the Hobby-Eberly Telescope. Subsequent testing revealed two limitations to SAMS ability to maintain the HET primary mirror figure: inadequate edge sensor temperature compensation and inadequate global radius of curvature compensation. Despite these limitations, testing over a 98.5-hour period revealed that the SAMS was capable of maintaining the sub-array mirror figure within specification within a 6-degree-C temperature band. The full potential of SAMS capability was demonstrated when the telescope was pointed at and tracked a celestial target for one hour. SAMS maintained a seeing-limited image quality for the duration of the observation. Work is in progress to improve the edge sensor temperature compensation and improve global radius of curvature compensation. Results thus far indicate that the SAMS concept, architecture and hardware are a viable practical approach to maintaining the primary mirror figures of large segmented telescopes.

ACKNOWLEDGEMENTS

The authors wish to thank Dr. Mark Adams, Superintendent of McDonald Observatory and SAMS Project Manager, for his patience, support and provision of precious engineering time. We also wish to thank John Booth, HET project engineer, and Dr. Larry Ramsey, HET project scientist, for their guidance and encouragement. We want to extend special thanks to the HET staff which supported SAMS installation and testing: Jim Fowler, Craig Nance, Matthew Shetrone, Brian Roman, Teddy George, Vicki Riley and Ben Laws.

REFERENCES

1. Ramsey, L.W., Adams, M.T., Barnes, T.G., Booth, J.A., Cornell, M.E., Fowler, J.R., Gaffney, N., Glaspey, J.W., Good, J., Kelton, P.W., Krabbendam, V.L., Long, L., Ray, F.B., Ricklefs, R.L., Sage,J., Sebring, T.A., Spiesman, W.J., & Steiner, M., 1998, "The early performance and present status of the Hobby-Eberly Telescope," S.P.I.E. Vol. 3352, Advanced Technology Optical/IR Telescope VI, p.34.
2. J.W. Glaspey, M.T. Adams, J.A. Booth, M.E. Cornell, J.R. Fowler, V.I. Krabbendam, L.W. Ramsey, F.B. Ray, R.L. Ricklefs, and W.J. Spiesman, 1998, "Hobby-Eberly Telescope: commissioning experience and observing plans," S.P.I.E. Vol. 3349, Observatory Operations to Optimize Scientific Return, p.50.
3. Montgomery, E., Ames, G., Rakoczy, J., Weir, J., Lindner, J., "A Proposal for a Segment Alignment Maintenance System, Hobby-Eberly Telescope," August 3, 1999.
4. J. Booth, M. Adams, G. Ames, J. Fowler, E. Montgomery, J. Rakoczy, "Development of the Segment Alignment Maintenance System (SAMS) for the Hobby-Eberly Telescope," No. 4003-20, SPIE: Astronomical Telescopes and Instrumentation 2000, March 27-31, 2000, Munich, Germany.
5. J. Rakoczy, E. Montgomery, J. Lindner, "Recent Enhancements of the Phase Array Mirror Extendible Large Aperture (PAMELA) Telescope Testbed at MSFC," No. 4004-61, SPIE: Astronomical Telescopes and Instrumentation 2000, March 27-31, 2000, Munich, Germany.